Molecular Biology of the Cell
Vol. 5, 807–818, July 1994

Yeast Mitochondria Contain ATP-sensitive, Reversible Actin-binding Activity

Deborah A. Lazzarino,* Istvan Boldogh,* Michael G. Smith, Jonathan Rosand, and Liza A. Pon

Department of Anatomy and Cell Biology, Columbia University College of Physicians and Surgeons, New York, New York, 10032

Submitted March 16, 1994; Accepted June 16, 1994
Monitoring Editor: Gottfried Schatz

Sedimentation assays were used to demonstrate and characterize binding of isolated yeast mitochondria to phalloidin-stabilized yeast F-actin. These actin-mitochondrial interactions are ATP sensitive, saturable, reversible, and do not depend upon mitochondrial membrane potential. Protease digestion of mitochondrial outer membrane proteins or saturation of myosin-binding sites on F-actin with the S1 subfragment of skeletal myosin block binding. These observations indicate that a protein (or proteins) on the mitochondrial surface mediates ATP-sensitive, reversible binding of mitochondria to the lateral surface of microfilaments. Actin copurifies with mitochondria during subcellular fractionation and is released from the organelle upon treatment with ATP. Thus, actin-mitochondrial interactions resembling those observed in vitro may also exist in intact yeast cells. Finally, a yeast mutant bearing a temperature-sensitive mutation in the actin-encoding *ACT1* gene (*act1-3*) displays temperature-dependent defects in transfer of mitochondria from mother cells to newly developed buds during yeast cell mitosis.

INTRODUCTION

The actin cytoskeleton of *Saccharomyces cerevisiae* consists of cytoplasmic cables and peripherally arranged patches (Adams and Pringle, 1984; Kilmartin and Adams, 1984). Analyses of both the distribution of actin within yeast cells and the effect of mutation of the single, essential, actin-encoding *ACT1* gene (Ng and Abelson, 1980; Shortle *et al.*, 1982) indicate that the actin cytoskeleton is involved in numerous aspects of cellular function. These include polarized cell growth (Adams and Pringle, 1984; Kilmartin and Adams, 1984; Drubin *et al.*, 1993), mating projection formation (Read *et al.*, 1992), bud separation during cytokinesis (Novick and Botstein, 1985), control of spindle position during anaphase (Palmer *et al.*, 1992), response to osmotic stress (Chowdhury *et al.*, 1992), control of mitochondrial position (Drubin *et al.*, 1993), as well as vesicle movement during bud expansion, early stages of endocytosis, and late stages of secretion (Govindan *et al.*, 1991; Johnston *et al.*, 1991; Riezman, 1993). In this study, we explored the basis of actin-dependent control of mitochondrial position in yeast and the possible role of the actin cytoskeleton in mitochondrial inheritance during cell division.

Actin-dependent movement of organelles and vesicles has been observed in *Acanthamoeba, Chara, Dictyostelium,* cultured fibroblasts, and squid axon (Kachar, 1985; Adams and Pollard, 1986; Kachar and Reese, 1988; Wessels *et al.*, 1989; Hegmann *et al.*, 1990, 1991; and Kuznetsov *et al.*, 1992). The current model proposes that myosins, a family of actin-dependent motor molecules, bind to both the microfilament and the organelle and utilize the energy of ATP hydrolysis to drive organelle movement along cytoskeletal tracks. This model is based on findings that 1) muscle and nonmuscle myosins are capable of driving ATP-dependent particle movement along actin filaments (Sheetz and Spudich, 1983; Albanesi *et al.*, 1985), 2) proteins that are immunologically cross-reactive with myosin are associated with vesicles and organelles that bind to or move along microfilaments (Burridge and Phillips, 1975; Grolig *et al.*, 1988; Fath and Burgess, 1993), 3) antibodies raised against myosin block organelle movement along actin bundles in vitro (Adams and Pollard, 1986), and 4) mu-

* The first and second authors (D.A.L. and I.B.) contributed equally to the work presented.

tations in myosin genes inhibit particle movement in *Dictyostelium* and budding yeast (Wessels and Soll, 1990; Govindan *et al.*, 1991; Johnston *et al.*, 1991).

Recently, a second mechanism of actin-driven particle movement was observed in *Listeria monocytogenes*–infected macrophages (Tilney *et al.*, 1992a,b) and in lanthanum- and zinc-treated cells (Heuser and Morisaki, 1992). In these studies, bacteria and endosomes "rocket" through the cytoplasm with the particle or bacterium leading and a tail consisting of short actin filaments trailing behind. Forward motion appears to be driven by nucleation of actin polymerization by proteins on the surface of the particle and insertion of actin monomers at the base of the moving particle (Theriot *et al.*, 1992).

Using subcellular fractionation analysis and sedimentation assays to examine organelle-cytoskeleton binding, we present evidence for specific direct interactions between yeast mitochondria and actin filaments. Analysis of the functional significance of these interactions focused on the distribution of actin and mitochondria in yeast and the effect of an actin mutation on mitochondrial distribution and inheritance. Previous studies indicate that mitochondrial inheritance, the transfer of mitochondria from mother cells to buds during mitosis, begins shortly after bud emergence (Stevens, 1977, 1981). Because mitochondria are essential organelles that are produced from preexisting mitochondria, this transfer process is necessary to produce viable progeny during cell division. Recent studies indicate that mitochondrial inheritance is blocked in temperature sensitive mitochondrial distribution mutants (*mdm1* and *mdm2*) (McConnell *et al.*, 1990) and that this process occurs in the absence of microtubule function (Huffacker *et al.*, 1988) and nuclear division (Thomas and Botstein, 1986). Other studies suggest a role for actin in control of mitochondrial position. Drubin *et al.* (1993) observe alignment of mitochondria along yeast actin cables and find that mutants bearing charged amino acid to alanine substitutions in the actin-encoding *ACT1* gene contain abnormal clumps of mitochondria. Here, we examined the effect of one of the original *ACT1* mutations, the *act1-3* allele (Shortle *et al.*, 1984), on mitochondrial distribution and inheritance during yeast cell mitosis. The *act1-3* mutation is a temperature-sensitive lethal mutation produced by substitution of leucine for proline at position 32 within subdomain 2 of the *ACT1* gene product. This mutation results in temperature-dependent defects in mitochondrial distribution and inheritance.

MATERIALS AND METHODS

Yeast Strains

Yeast cell growth, matings, sporulation, and analysis by tetrad dissection were carried out according to Sherman (1991). The effect of the *act1-3* mutation on mitochondrial spatial arrangement was analyzed using the temperature sensitive actin mutants *DBY1691* (*MATa, his4-619, act1-3*) (Shortle *et al.*, 1984) and *KWY230* (*MATa/α, his3Δ200/hisΔ200, ura3-52/ura3-52, lys2-801/LYS2, act1-3/act1-3, LEU2/leu2-3,112*) and the wild-type strains *KWY474* (*MATa/α, tub2-201/tub2-201*) (a mutation that confers benomyl resistance on microtubules), *his3Δ200/his3Δ200, ura3-52/ura3-52, leu2-3,112/leu2-3,112, ADE2/ade2-101, CRY1/cry1, ade4/ADE4*), *DBY877* (*MATα, his4-619*), and *W303-1B* (*MATα, ade2-1, trp1-1, his3-11,15, can1-100, ura3-1, leu2-3,112*). *D273-10B* (*MATα*, ATCC25657) was used for mitochondrial isolation.

Mitochondrial Preparation

The wild-type yeast strain *D273-10B* was grown to midlog phase in lactate medium. Cells were harvested, washed, and converted to spheroplasts in zymolyase-catalyzed reactions as described previously (Daum *et al.*, 1982). Using invertase secretion as an indicator of cellular activity, Baker and Schekman (1989) have reported that the conditions routinely used for spheroplast production compromise yeast metabolism. Therefore, to restore metabolic activity, spheroplasts were "regenerated" using a modification of published methods (Baker and Schekman, 1989). Spheroplasts were concentrated by centrifugation (2000 × *g*, 10 min at 4°C) and incubated at a concentration of 10^6 cells/ml in 1.2 M sorbitol, 0.3% (wt/vol) yeast extract, 0.05% (wt/vol) $CaCl_2$, 0.05% (wt/vol) NaCl, 0.06% (wt/vol) $MgCl_2$, 0.1% (wt/vol) NH_4Cl, 2% (vol/vol) lactate pH 5.5 for 45 min at 30°C. Regenerated spheroplasts were then isolated by centrifugation (2000 × *g*, 10 min at 4°C) and resuspended in breaking buffer (0.6 M sorbitol, 20 mM *N*-2-hydroxyethylpiperazine-*N*-2-ethanesulfonic acid [HEPES]-KOH pH 7.4) containing a protease inhibitor cocktail (1 mM phenylmethylsulfonyl fluoride [PMSF], 10 mM benzamidine, 1 mg/ml 1,10-phenanthroline, 0.5 mg/ml antipain, 0.5 mg/ml chymostatin, 0.5 mg/ml leupeptin, 0.5 mg/ml pepstatin, and 0.5 mg/ml aprotinin). Spheroplasts were disrupted using a Dounce homogenizer (Wheaton, Millville, NJ). Crude mitochondria were isolated from the homogenate by differential centrifugation as described previously (Daum *et al.*, 1982).

Further purification of the crude mitochondrial fraction was carried out by isopycnic centrifugation using Nycodenz (5-(N-2,3-Dihydroxypropylacetamido-2,4,6-triiodo-N,N'-bis(2,3-dihydroxy-propyl) isophthalamide) (Sigma, St. Louis, MO) gradients. The gradients consisted of linear gradations of 5–25% (wt/vol) Nycodenz in breaking buffer containing the protease inhibitor cocktail described above. Crude mitochondria were separated from residual cell debris, mitoplasts, and lipids by centrifugation at 75 000 × *g* for 90 min at 4°C. In the subcellular fractionation study and many of the actin-binding assays described below, Nycodenz-purified mitochondria were used immediately after fractionation. Some of the binding studies were carried out using mitochondria that had been stored in liquid nitrogen at a concentration of 5–10 mg/ml in isoosmotic Nycodenz/breaking buffer solutions and thawed at 30°C immediately before use. The purity of the mitochondrial preparation was evaluated by Western blot analysis using polyclonal antibodies raised against cytochrome b_2, *Sec61p* (Stirling *et al.*, 1992), and *Gas1p* (Nuoffer *et al.*, 1993). Nuclear envelope contaminants were identified using MAb414, a monoclonal antibody raised against nuclear pore complex (BAbCo).

Protein Purification

Preparation of Yeast Actin. Actin was isolated according to Zechel (1980) and Drubin *et al.* (1988). To do so, blocks of fresh baker's yeast were suspended in buffer G (2 mM tris-(hydroxymethyl)aminomethane [Tris]-HCl pH 7.5, 0.2 mM ATP, and 0.2 mM $CaCl_2$) containing the protease inhibitor cocktail described above and were disrupted by three 1-min bursts with 0.5-mm glass beads using a Bead-Beater homogenizer (Biospec Products, Bartlesville, OK) on ice. Homogenates were clarified by centrifugation at 100 000 × *g* for 1.5 h at 4°C and filtered through cheese cloth. After addition of dithiothreitol (DTT) to a final con-

centration of 1 mM, the homogenate was applied to a column of DNase 1 (Boehringer Mannheim, Indianapolis, IN) coupled to CNBR-activated Sepharose 4B (Pharmacia, Piscataway, NJ). Nonspecifically bound material was removed by washes with buffer G containing 0 and 10% formamide. Thereafter, bound actin was eluted with buffer G containing 40% formamide. Formamide was removed from the crude actin solution by dialysis against buffer G overnight at 4°C, and G-actin was concentrated by ultrafiltration also at 4°C. Crude actin was further purified by two rounds of polymerization and depolymerization. Actin was polymerized by addition of $MgCl_2$, KCl, and ATP to final concentrations of 2, 50, and 1 mM, respectively, to a solution of G-actin in buffer G. After incubation of the sample at 4°C for 1 h, F-actin was separated from low density contaminants by centrifugation at 175 000 × *g* for 20 min at 4°C. For depolymerization, F-actin was dialyzed against buffer A (2 mM Tris-HCl pH 8.0, 0.2 mM $CaCl_2$, 0.2 mM ATP, and 0.5 mM DTT) for 36 h. Protein concentrations were determined by the Bicinchoninic Acid (BCA) Protein Assay (Pierce, Rockford, IL).

Preparation of Myosin Subfragment-1. Rabbit white muscle myosin was purified as described by Sreter *et al.* (1972). In our preparation, the column purification step was omitted. Myosin subfragment-1 (S1) was prepared by chymotryptic digestion of purified muscle myosin according to Weeds and Taylor (1975). To remove high-molecular-weight contaminants, S1 was further purified by gel filtration chromatography using a Sephadex G-100 column (1 × 60 cm) equilibrated with 0.1 M KCl, 20 mM imidazole pH 7, 1 mM DTT, and 1 mM EDTA.

Analysis of Mitochondrial-Actin Interactions In Vitro

Preparation of Phalloidin-stabilized F-Actin. The phalloidin-stabilized F-actin used for these studies was prepared by incubating G-actin (1 mg/ml) with phalloidin (10 μg/ml) (Boehringer Mannheim), $MgCl_2$ (4 mM), ATP (1 mM), and KCl (50 mM) in buffer A for 1 h at 4°C. Actin filaments were isolated by centrifugation at 175 000 × *g* for 30 min at 4°C using a TL100.3 rotor in a Beckman TL-100 tabletop ultracentrifuge (Fullerton, CA). Newly polymerized actin was suspended in RM (0.6 M sorbitol, 20 mM HEPES-KOH pH 7.4, 100 mM KCl, 5 mM $MgCl_2$, 1 mM DTT, 1 mg/ml fatty acid-free bovine serum albumin [BSA], and the protease inhibitor cocktail described above) and clarified by centrifugation at 12 500 × *g* for 30 min at 4°C. The material recovered in the supernatant of this centrifugation was used to evaluate the ATP-sensitive actin-binding activity in isolated mitochondria. For the experiments evaluating the reversibility of actin-mitochondrial interactions (Figure 7), ATP was depleted from phalloidin-stabilized F-actin by incubation with hexokinase-agarose (10 U/ml) (Sigma), 2 mM glucose, and 3 mM $MgCl_2$ for 15 min at 4°C. Thereafter, agarose-immobilized hexokinase was separated from the reaction mixture by centrifugation at 12 500 × *g* for 5 min, and residual F-actin that adhered to the agarose beads was eluted by 3 washes with RM. The ATP-depleted F-actin was then pooled and clarified as described above.

Binding Conditions. Isolated yeast mitochondria (2 mg/ml) were incubated with phalloidin-stabilized F-actin (3.3–12 μM) for 10 min at 30°C in 100 μl of RM. In ATP-treated samples, ATP levels were maintained at 2 mM by addition of ATP and an ATP-regenerating system (0.1 mg/ml creatine kinase and 10 mM creatine phosphate). To deplete the system of ATP, apyrase (type VI, Sigma) was added to a final concentration of 12.5 U/ml (Pon *et al.*, 1989). In all cases, ATP was either added or depleted from the reaction mixture before the addition of mitochondria. In some cases, valinomycin (5 μg/ml) was added to dissipate mitochondrial membrane potential (Tzagoloff, 1982). Subsequent to binding, mitochondria were separated from unbound actin filaments by centrifugation through a sucrose cushion (25% sucrose in 20 mM HEPES-KOH pH 7.4) at 12 500 × *g* for 10 min. Proteins recovered in the mitochondrial pellet and in the supernatants were separated by sodium dodecyl sulfate-polyacrylamide gel electrophoresis (SDS-PAGE) (Laemmli, 1970) and identified by Western blot analysis (Towbin *et al.*, 1979) using polyclonal antibodies raised against the mitochondrial marker proteins cytochrome b_2 and porin (gifts from G. Schatz) and monoclonal anti-actin antibodies (c4d6) (Lessard, 1988). Visualization of antigen-antibody complexes was carried out using horseradish peroxidase-coupled secondary antibodies (Kirkegaard and Perry Laboratories Gathersburg, MD) and the electrochemiluminescence (ECL) Western blot detection kit (Amersham, Arlington Heights, IL). In one case, affinity-purified, alkaline phosphatase-coupled goat anti-rabbit antibodies (Promega, Madison, WI) and the colorimetric alkaline phosphatase substrates, bromochloroindoyl phosphate and nitro blue tetrazolium (Harlow and Lane, 1988), were used for detection.

Scanning Densitometry. The images of bands detected on fluorograms for immunoblots were acquired by UMax 600 transmission scanner using Adobe Photoshop program (v. 2.5) on a Macintosh Quadra 800 computer (Apple Computer, Cupertino, CA). National Institutes of Health (NIH) Image Program (v. 1.49) was used for analyzing images; an appropriate selection was made that covers each of the individual bands and computes their mean gray values. These measurements were allowed to evaluate relative quantities of proteins. For quantitation of actin binding, the density of the band of actin recovered in the mitochondrial pellet was compared with the densities of known amounts of actin standards on the same gel.

Analysis of Mitochondrial Distribution in Intact Yeast Cells

Preparation of Cell Samples. Yeast cell fixation and preparation for fluorescence microscopy followed a modification of published procedures (Pringle *et al.*, 1989). Midlog-phase yeast cells (0.5–1.5 OD_{600}) were fixed by addition of formaldehyde and potassium phosphate buffer (KPi) pH 6.5 directly to culture medium to final concentrations of 5% and 125 mM, respectively. After fixation for 15 min, yeast were isolated by centrifugation (1000 × *g* for 10 min). Further fixation was achieved by incubation in 0.1 M KPi pH 6.5, 2 mM $MgCl_2$, 5% formaldehyde at room temperature (RT) for 1 h. Fixed cells were washed with wash solution (25 mM KPi pH 7.5, 0.8 M KCl). To remove cell walls, samples were pretreated with wash solution containing 10 mM DTT for 20 min at 30°C and then incubated at a concentration of 9 × 10^8 cells/ml in wash solution containing 0.25 mg/ml zymolyase 20T (ICN, Costa Mesa, CA) for 2.5 h at 30°C. Zymolyase was then removed by washes with NS (20 mM Tris-HCl pH 7.6, 0.25 M sucrose, 1 mM EDTA, 1 mM $MgCl_2$, 0.1 mM $ZnCl_2$, 0.1 mM $CaCl_2$).

Fluorescence Microscopy. The method used for indirect immunofluorescence is a modification of published methods (Pringle *et al.*, 1989). Fixed spheroplasts were applied to polylysine-coated coverslips and allowed to adhere to the coverslips for 20 min. Immobilized spheroplasts were then gently washed in phosphate-buffered saline (PBS) and incubated in PBT (1 × PBS, 0.1% [vol/vol] Triton X-100, 0.02% [vol/vol] sodium azide, 1% [wt/vol] BSA) for 5 min at room temperature. This was followed by incubation with primary antibody for 2 h at RT. All incubation steps were carried out in a humid chamber in the dark. Rabbit polyclonal antiserum raised against total mitochondrial outer membrane proteins was utilized to visualize mitochondrial membranes. The anti-outer membrane antibody was prepared by immunizing rabbits with mitochondrial outer membranes, as described previously (Riezman *et al.*, 1983). Analysis of the polyclonal antiserum using Western blots indicates that the antibody recognizes several proteins including all of the major outer membrane proteins (porin, MAS 70, and the 33- and 45-kDa outer membrane proteins). Because all antigens recognized by the antiserum are present in mitochondria, depleted in mitochondrial inner membrane vesicles, and enriched in preparations of mitochondrial outer membrane vesicles, the antiserum appears to be specific for the mitochondrial outer membrane. The antiserum was preadsorbed with intact yeast cells before use.

Subsequent to incubation with primary antibodies, spheroplasts were washed with PBT and incubated with fluorescently labeled sec-

ondary antibody for 30–60 min at RT. The secondary antibody used for these studies, fluorescein isothiocyanate-coupled goat anti-rabbit IgG (Boehringer Mannheim), was reconstituted, stored, and used according to the manufacturer's instructions. The spheroplasts were washed with PBS to remove unbound secondary antibody and mounted on microscope slides using mounting solution (1 mg/ml *p*-phenylenediamine, 90% [wt/vol] glycerol, and 1× PBS). For some experiments mounting solution was supplemented with the DNA binding dye 4,6-diamidino-2-phenylindole (DAPI) (Williamson and Fennell, 1975) at a final concentration of 1 μg/ml. Coverslips were then sealed onto glass microscope slides with clear nail polish. Slides were stored at −20°C in the dark before viewing with a Leitz Diaphot fluorescence microscope (Rockleigh, NJ) equipped with 3.1× or 2× projection lenses (National Diagnostics, Manville, NJ) and a controlled shutter drive (Uniblitz D122, Vincent Associates, Rochester, NY). Images were collected using a Star-1 cooled CCD camera (Photometric, Tucson, Arizona), enhanced using NIH Image (v. 1.49), and stored on a Macintosh Quadra 800 equipped with a Magnetic Optical Disk Drive (Peripheral Land, Fremont, CA).

The actin cytoskeleton was visualized using rhodamine-coupled phalloidin (Molecular Probes, Eugene, OR), a ligand that binds specifically to actin polymers (Cooper, 1987), using published protocols (Pringle *et al.*, 1989). The fluorescent ligand was added to fixed spheroplast samples to a final concentration of 2.5 μM in a solution consisting of a 4:1 ratio of NS to methanol, and samples were allowed to stand in the dark at 4°C for 16 h. Thereafter, the mixture was diluted with a threefold excess of PBS and applied directly to polylysine-coated coverslips. Immobilized rhodamine phalloidin-stained spheroplasts were also stained for mitochondrial DNA, as described above.

RESULTS

ATP-Sensitive Actin-binding Activity in Isolated Yeast Mitochondria

Previous studies indicate that myosin, the actin-associated motor molecule, mediates association and movement of organelles along microfilaments in neuronal and nonneuronal cells (see above). Because this interaction is sensitive to Mg^{+2}-ATP, we examined the effect of ATP on interaction of mitochondria with F-actin using a sedimentation assay. Isolated yeast mitochondria were incubated with phalloidin-stabilized yeast actin filaments. Mitochondria were then separated from the reaction mixture by low-speed centrifugation, and the amount of actin that sedimented with the organelle fraction was determined using Western blots. As shown in Figure 1A, incubation of F-actin with mitochondria under conditions of ATP depletion results in cosedimentation of actin with mitochondria (lane 4). In contrast, F-actin is not detected in any significant levels within low-speed pellets after incubation in mitochondria-free mixtures (lanes 1–2) or in reaction mixtures containing mitochondria and ATP (lane 3). As a result of decline in activity upon storage of microfilament and mitochondrial preparations, the amount of actin that sediments with ATP-depleted mitochondrial preparations varied among experiments. However, analysis of the recovery of actin with the mitochondrial marker proteins, cytochrome b_2 and porin, indicates that addition of ATP results in a 13- to 54-fold (n = 14) decrease in the amount of actin associated with the organelle pellet.

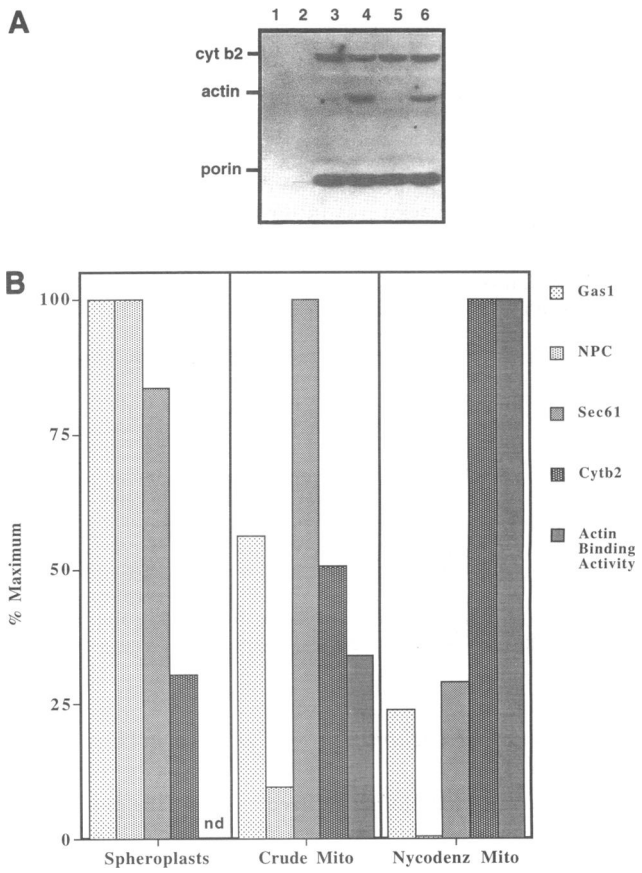

Figure 1. ATP-sensitive actin-mitochondrial interactions in vitro. (A) Isolated yeast mitochondria (2 mg/ml) were incubated with 3.3 μM of phalloidin-stabilized F-actin with ATP and an ATP regenerating system or with apyrase as described in MATERIALS AND METHODS. After incubation for 10 min at 30°C, mitochondria were separated from each reaction mixture by centrifugation through a sucrose cushion (12 500 × *g*, 10 min, 4°C). The levels of actin and of two mitochondrial marker proteins (cytochrome b_2 and porin) were evaluated in the pellets of the sedimented reaction mixtures by Western blot analysis. Actin was detected using a monoclonal anti-actin antibody. Recovery of the mitochondrial marker protein cytochrome b_2 was determined by redecoration of the Western blot with a polyclonal anti-cytochrome b_2 antibody. Lanes 1 and 2: sedimented material recovered from mitochondria-free reactions incubated in the presence or absence of ATP, respectively. Lanes 3 and 4: mitochondrial pellets from complete reactions after incubation in the presence or absence of ATP, respectively. Lanes 5 and 6: mitochondrial pellets after incubation of organelles treated with valinomycin (1 μg/ml) in complete reaction mixtures in the presence or absence of ATP, respectively. (B) The levels of the membrane marker proteins, *Sec61p*, *Gas1p*, nuclear pore complex proteins, and cytochrome b_2 were evaluated in spheroplasts, crude mitochondria, and Nycodenz-purified mitochondria by Western blot analysis, using the ECL detection system. The density of the bands was quantitated by scanning densitometry. In all cases, protein load and visualization of antibody antigen complex allowed for quantitation of proteins within the linear range of detectability. For each marker protein, 100% was defined as the maximum amount of marker per mg of total protein. ATP-sensitive actin binding activity per mg protein in the crude and Nycodenz-purified mitochondria was determined as described in A and defined as the ratio of actin bound in ATP-depleted samples to that in ATP-containing samples. Here too, 100% was defined as the amount of binding activity in the sample containing the highest specific activity. nd, not done.

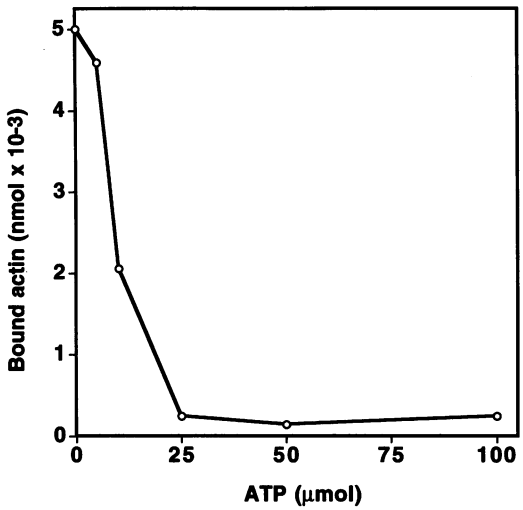

Figure 2. The effect of ATP concentration on binding of F-actin to isolated yeast mitochondria. Valinomycin-treated mitochondria (2 mg/ml) were incubated with ATP-free, phalloidin-stabilized F-actin (3.5 μM) and 0–100 μM ATP for 10 min at 30°C. Mitochondria were then isolated, and actin cosedimenting with mitochondria was identified by Western blot analysis as described in Figure 1. The amount of actin was measured by densitometric scans of the fluorograms from immunoblots and by comparison of band densities of organelle-associated actin with those of known quantities of actin. The results shown are representative of four independent ATP titration studies.

Mitochondria used in the sedimentation assay were isolated by differential centrifugation and further purified by Nycodenz gradient centrifugation. To confirm that sedimentation of actin with the organelle pellet was not because of cytosolic or membrane contaminants, we compared the fractionation pattern of actin-binding activity with that of membrane marker proteins (Figure 1B). The marker proteins evaluated include cytochrome b_2, a peripheral membrane mitochondrial protein; *Gas1p*, a glycosylphosphatidylinositol-anchored protein that is transported through the endoplasmic reticulum (ER), Golgi apparatus, and secretory vesicles before insertion into the plasma membrane (Nuoffer *et al.*, 1993); *Sec61p*, an integral membrane protein within the ER (Stirling *et al.*, 1992); and proteins from nuclear pore complex (Davis and Blobel, 1986). Membrane contaminants are present in crude mitochondria. Upon further purification using the Nycodenz gradient, we observe an enrichment of the mitochondrial marker and removal of the other membranes examined. In addition, Nycodenz gradient centrifugation effectively separates mitoplasts (mitochondria with ruptured outer membranes) from mitochondria. This increase in both the purity and quality of mitochondria correlates with an enrichment in the ATP-sensitive actin-binding activity. Thus, the ATP-sensitive actin-binding activity detected in the isolated organelles resides in mitochondria and not in membrane contaminants within the mitochondrial preparation.

Further analysis of mitochondrial-actin interactions focused on the role of ATP and mitochondrial membrane potential on actin-mitochondrial interactions. Mitochondria were treated with the potassium ionophore valinomycin before addition to the binding reaction. As expected, actin does not sediment with valinomycin-treated mitochondria in the presence of ATP (Figure 1A, lane 5). However, upon depletion of ATP, actin-binding activity is recovered with ionophore-treated organelles. The amount of organelle-bound actin in valinomycin-treated samples is similar to that detected in the valinomycin-free control. Thus, the mitochondrial membrane potential does not appear to be essential for association of mitochondria with actin. To evaluate the concentration dependence of ATP-sensitive actin-mitochondrial interactions, the actin-binding activity of valinomycin-treated mitochondria was measured at different ATP concentrations. As shown in Figure 2, addition of 5–50 μM ATP results in an ATP dose-dependent decrease in actin-mitochondrial binding.

Actin-Mitochondrial Interactions Are Saturable and Reversible

In the studies above, binding was carried out using an excess of actin filaments, conditions under which 1–3% of the actin present in the ATP-depleted binding reaction is recovered in the organelle pellet. We examined the effect of actin concentration on the mitochondrial binding activity (Figure 3). In the presence of low levels of actin, as much as 19% of the actin sediments was present in the organelle pellet. Upon incubation with

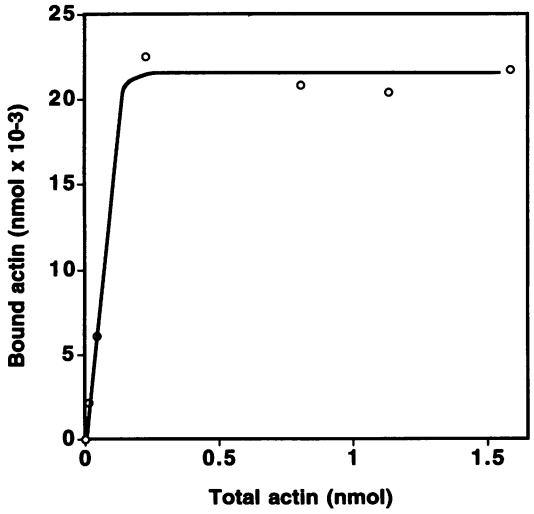

Figure 3. The effect of actin concentration on actin-mitochondrial interactions. Isolated mitochondria were incubated at 30°C for 10 min with 0–17.8 μM of phalloidin-stabilized F-actin. The amount of actin cosedimenting with mitochondria was measured as for Figure 2. The results shown are representative of three independent actin titration studies.

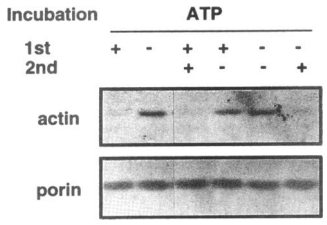

Figure 4. Actin-mitochondrial interactions are reversible. Mitochondria were incubated for 10 min (first incubation) with phalloidin-stabilized F-actin at 30°C in the presence or absence of ATP. Aliquots from the ATP-containing reaction mixture (+ATP) were incubated for an additional 10 min (second incubation) without additions (+ATP) or with apyrase (−ATP). Similarly, aliquots from the ATP-free reaction (−ATP) were incubated without additions (−ATP) or with ATP and an ATP-regenerating system (+ATP). Mitochondria were then isolated by centrifugation, and actin recovered in the mitochondrial pellet was detected as for Figure 1.

increasing amounts of actin, the amount of actin recovered in the mitochondrial pellet increases linearly and reaches a plateau. Because the number of occupied ligand binding sites on F-actin and on mitochondria is not known, these experiments do not provide any information regarding the affinity of F-actin for mitochondria. Nonetheless, these studies indicate that binding of microfilaments to mitochondria is both saturable and dependent on F-actin concentration, suggesting a limited number of specific actin-binding sites on the mitochondrial surface.

To evaluate the reversibility of these cell-free actin-mitochondrial interactions, mitochondria and phalloidin-stabilized F-actin were preincubated in the absence ATP for 10 min. Thereafter, ATP was added to an aliquot of the ATP-free mixture, and the actin binding activity of each mitochondrial sample was tested (Figure 4). Because essentially equal amounts of actin are bound to mitochondria after incubation for 10 or 20 min in ATP-free reactions, maximal binding occurs within 10 min of incubation. Under these conditions, addition of ATP to the ATP-free reaction releases F-actin from mitochondria. Similarly, removal of ATP from mixtures of F-actin and mitochondria results in association of microfilaments with the organelle. These findings indicate that ATP-sensitive actin-mitochondrial interactions are reversible.

Actin-Mitochondrial Interactions Are Inhibited by Protease Treatment of Mitochondria and by Pretreatment of F-Actin with Myosin Subfragment-1

Antibody inhibition has been used to examine the role of specific proteins in the association of mitochondria with F-actin. However, because all rabbit IgG preparations tested bind nonspecifically to yeast F-actin, this method is not readily compatible with our sedimentation assay. To examine the role of mitochondrial surface proteins in actin-mitochondrial interactions, we measured actin-binding in protease-treated mitochondria (Figure 5). Pretreatment with trypsin produces a quantitative loss of an outer membrane protein (*MAS 70*) and quantitative recovery of an intermembrane space protein (cytochrome b_2). Thus, the level of protease used in these experiments degrades mitochondrial surface proteins without affecting the integrity of the organelle. Under these conditions, there was no significant actin-binding activity in trypsin-treated mitochondria.

The myosin S1 fragment, the globular head domain of myosin, is responsible for ATP-sensitive binding to the lateral surface of the F-actin and is required for myosin motor activity (Vibert and Cohen, 1988; Holmes *et al.*, 1990). Because rabbit skeletal myosin S1 binds to yeast actin (Greer and Schekman, 1982) and is capable of driving ATP-dependent sliding of yeast F-actin (Kron *et al.*, 1992), chymotryptic S1 subfragment was used to characterize F-actin-mitochondrial interactions. Phalloidin-stabilized F-actin was incubated with a 1:1 molar ratio of S1, and possible association between mitochondria and S1/F-actin complexes was tested using the sedimentation assay (Figure 6). In control S1-free reaction mixtures, ATP-sensitive actin-binding activity is present in isolated mitochondria. In contrast, ATP-depleted mitochondria fail to show significant binding

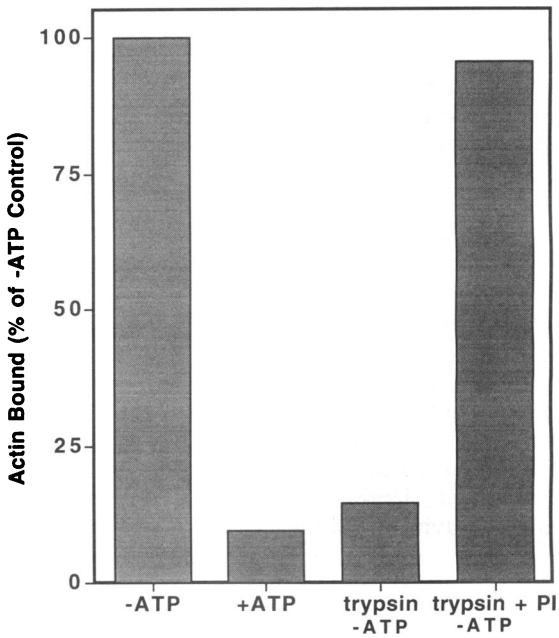

Figure 5. The effect of trypsin treatment on actin binding to mitochondria. Aliquots of freshly prepared mitochondria (2.5 mg/ml) were pretreated without additions, with 125 μg/ml trypsin, or with trypsin (125 μg/ml) and the protease inhibitors (PI) PMSF (1 mM) and soybean trypsin inhibitor (1 mg/ml). After incubation for 15 min at 4°C, active proteases were blocked by addition of PMSF (1 mM) and soybean trypsin inhibitor (1 mg/ml) and mitochondria were separated from the pretreatment reaction mixture by centrifugation through a sucrose cushion. Actin-binding activity of each mitochondrial sample was determined as for Figure 2. In all cases, the recovery of actin with the mitochondrial pellet was normalized for equal recovery of cytochrome b_2.

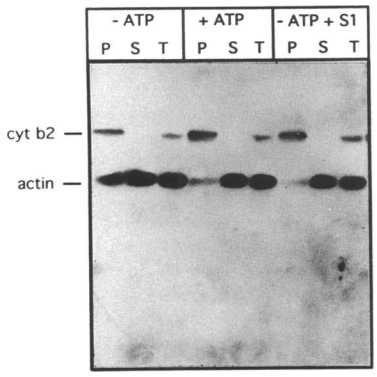

Figure 6. Mitochondria do not bind to S1-decorated actin filaments. Phalloidin-stabilized actin filaments (8 μM) were pretreated without any additions or with equimolar levels of purified myosin S1 fragments at 30°C for 30 min in RM buffer. Pretreated F-actin samples were then clarified by centrifugation as described in MATERIALS AND METHODS and added directly to the binding reaction mixture. Incubation of reaction mixtures upon addition (+ATP) or depletion of ATP (−ATP), and determination of the amount of actin recovered with mitochondria were carried out as for Figure 1. P, material recovered in the mitochondrial pellet; S, 5% of the material recovered in the supernatant; T, 5% of the total reaction mixture.

activity upon incubation with S1/F-actin complexes. Thus, pretreatment of yeast actin filaments with purified S1 inhibits microfilament-mitochondria complex formation.

Actin Copurifies with Mitochondria and Is Released from the Organelle upon Incubation with ATP

Here, we used subcellular fractionation to elucidate possible interactions between mitochondria and the actin cytoskeleton in vivo. Low levels of actin copurify with mitochondria after isolation by differential centrifugation and further purification by Nycodenz gradient centrifugation (Figure 7, lane 1). Because isolated mitochondria display ATP-sensitive actin-binding activity, we tested the effect of ATP treatment on actin-mitochondrial interactions in yeast subcellular fractions. Actin-mitochondrial complexes were incubated in the presence or absence of ATP, and material released from the organelle was separated from mitochondria by low speed centrifugation. Actin remains associated with the organelle upon incubation without additions (lane 2) or addition of the ATP trap, apyrase (lane 4). Less than 0.2% of the total cellular actin copurifies with mitochondria. Nonetheless, ~88% of the actin that copurifies with mitochondria is released from the ATP-treated organelle sample (lane 3). Our interpretation of these findings is that the actin-mitochondrial interactions observed upon cell fractionation are reversible and ATP-sensitive and therefore specific. Therefore the ATP-sensitive, reversible actin-mitochondrial interactions that are measured in the cell-free sedimentation assay appear similar to organelle-cytoskeletal interactions that may exist in living cells and persist through subcellular fractionation.

The act1-3 Mutant Displays Defects in Mitochondrial Position Control and Inheritance

Recent studies indicate that mutations in the actin-encoding *ACT1* yeast gene result in defects in mitochondrial organization (Drubin *et al.*, 1993). Here, we tested the effect of the *act1-3* mutation on mitochondrial distribution and inheritance (Figures 8 and 9). In the wild-type cell, mitochondrial threads and particles are present in the mother cells and in newly developed buds. Growth of the *act1-3* strain at semipermissive temperatures, however, results in enlarged cell size and multinucleation (Figure 8A, arrow). In addition, the *act1-3* strain displays defects in mitochondrial position similar to those observed in other actin mutants. DAPI staining of mitochondrial DNA shows that mitochondria are closely apposed, producing thick threads or ring patterns not observed in wild-type cells. In cases where aggregation is more pronounced, all of the mitochondrial DNA within a cell is located in one area. Double label studies using antibodies raised against mitochondrial outer membrane proteins indicate that the DAPI-stained cytoplasmic clumps also contain mitochondrial membranes (Figure 8A, panel D). Finally, ultrastructural analysis by transmission electron microscopy (unpublished data) reveals that mitochondria within the clumps are somewhat larger in size than those observed in wild-type cells. However, the overall shape and appearance of the individual organelles do not appear to be significantly affected.

This aggregation is also produced by short-term incubation of the mutant at elevated temperatures (Figure 8B). In wild-type cells there is a low level of mitochondrial aggregation that does not vary significantly with temperature. The *act1-3* mutant, however, shows widespread mitochondrial aggregation in budded and unbudded cells after short-term incubation at semipermissive or restrictive temperature. The number of cells containing mitochondrial aggregates increases as a

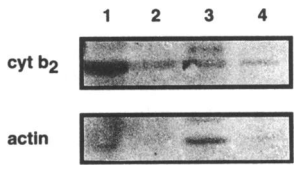

Figure 7. ATP-sensitive copurification of actin with mitochondria. Yeast mitochondria were isolated from the wild-type strain, *D273-10B*, by differential and Nycodenz gradient centrifugation. Mitochondria were incubated for 10 min at 30°C without additions, with ATP (2.5 mM), or with the ATP trap, apyrase (12.5 U/ml). Mitochondria were then separated from the reaction by low-speed centrifugation (12 500 × *g*, 10 min, 4°C), and proteins in the organelle pellet and supernatant were separated by SDS-PAGE. Lane 1, intact mitochondria (0.25 mg); lanes 2–4, soluble material released from 6 mg of mitochondria after incubation without additions (lane 2), with ATP (lane 3), or with apyrase (lane 4).

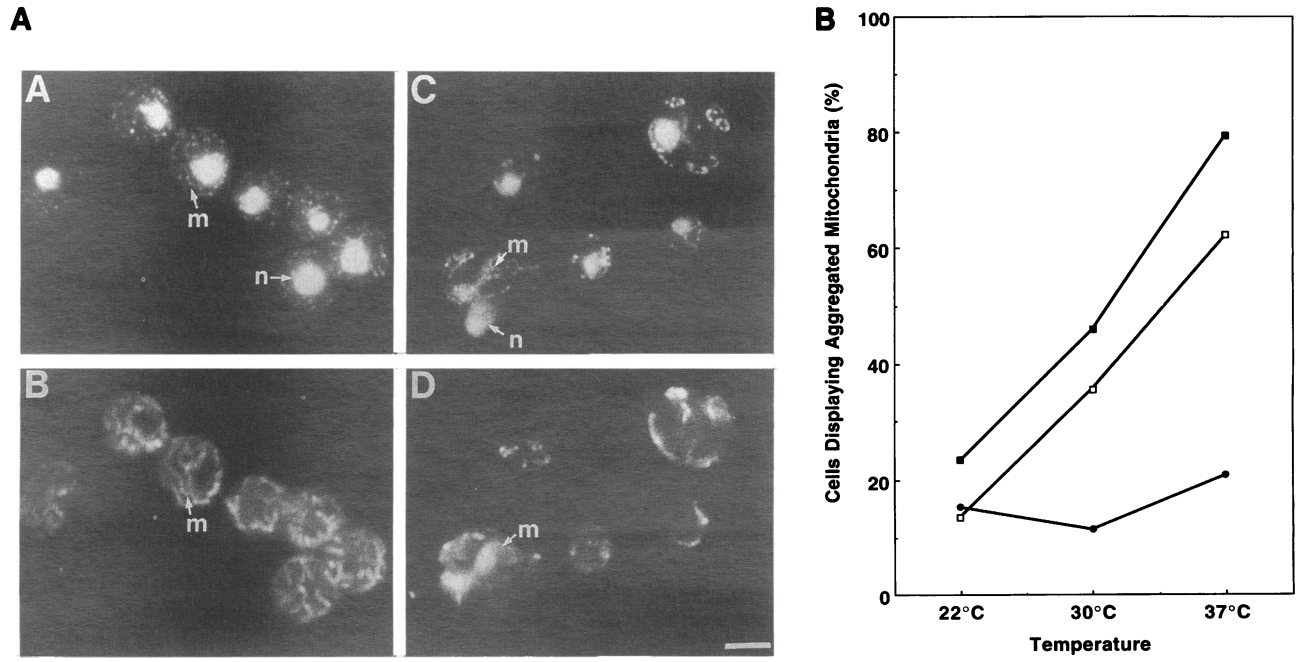

Figure 8. Effect of the *act1-3* mutation on mitochondrial distribution. (A) *DBY877* and *DBY1691*, yeast strains bearing wild-type and mutant forms of the *ACT1* gene, respectively, were grown to midlog phase in semisynthetic glucose-based media (YPD) at 29°C. Cells were fixed and converted to spheroplasts as described in MATERIALS AND METHODS. Mitochondria were visualized by indirect immunofluorescence using antibodies raised against total mitochondrial outer membrane proteins (B and D). Mitochondrial and nuclear DNA were visualized in the same cells using the DNA-binding dye DAPI (A and C). Mitochondria (m) and nuclei (n) are shown for the wild-type (A and B) and *act1-3* mutant (C and D). Bar, 2 μm. (B) *DBY877* and *DBY1691* were grown to midlog phase at a permissive temperature (22°C) in YPD. Aliquots of each strain were transferred to 22, 30, or 37°C for 1 or 2 h. Cells were fixed and converted to spheroplasts. Mitochondria were visualized using DAPI as for Figure 8A. Here, the percentage of cells exhibiting mitochondrial aggregates was determined as a function of temperature of incubation. ●, wild-type cells after incubation at 22, 30, or 37°C for 2 hrs; □ and ■, *act1-3* mutants after incubation at various temperatures for 1 and 2 h, respectively.

function of both time and temperature of incubation. Consistent with this, we observe that revertants, *act1-3*-derived cells that display temperature insensitive growth, also show wild-type mitochondrial arrangement (unpublished data). In addition, in eight tetrads analyzed, abnormal mitochondrial distribution segregates with the temperature-sensitive actin mutation in a manner independent of the *ade2* mutation. Thus, the mitochondrial aggregation is a consequence of the actin mutation.

During cell division, mitochondria are transferred from mother cells to developing buds. We examined the effect of the *act1-3* mutation on this transfer process. The distribution of actin and mitochondria during mitochondrial inheritance in wild-type cells is shown in Figure 9A. Mitochondria resolve as tubules that extend across the bud neck and are enriched in the bud tip. In the same cells, actin patches are concentrated within buds and actin cables are found mainly along the long axes between mother and developing daughter cells. Although the density of actin patches in buds precludes evaluation of possible actin-mitochondrial interactions, some mitochondria align along actin cables (arrows).

Previous studies indicate that mitochondrial inheritance begins shortly after bud emergence (Stevens, 1977, 1981). As shown in Table 1, mitochondria are present in ~85% of the small and medium sized buds in wild-type glucose-grown cells. The efficiency of mitochondrial inheritance is slightly higher during growth using lactate as a carbon source. In contrast, transfer of mitochondria into newly developed buds is compromised in the actin mutant. After growth at semipermissive temperatures, actin patches are present and enriched in buds, and mitochondria are present in mother cells but are absent or present in low levels in small and medium-sized buds (Figure 9B). Some cells display mitochondrial inheritance defects and mitochondrial aggregation (Figure 9B, left and right panels). Others (e.g., Figure 9B, center panels) show inheritance defects and low levels of mitochondrial aggregation. To characterize this effect further, we tested the effect of short-term temperature shifts on mitochondrial inheritance. During growth at permissive temperatures, there is some inhibition of mitochondrial inheritance in the actin mutant compared to the wild-type sister (Table 1). In these cells, inheritance defects occur in the absence of aggregation. In

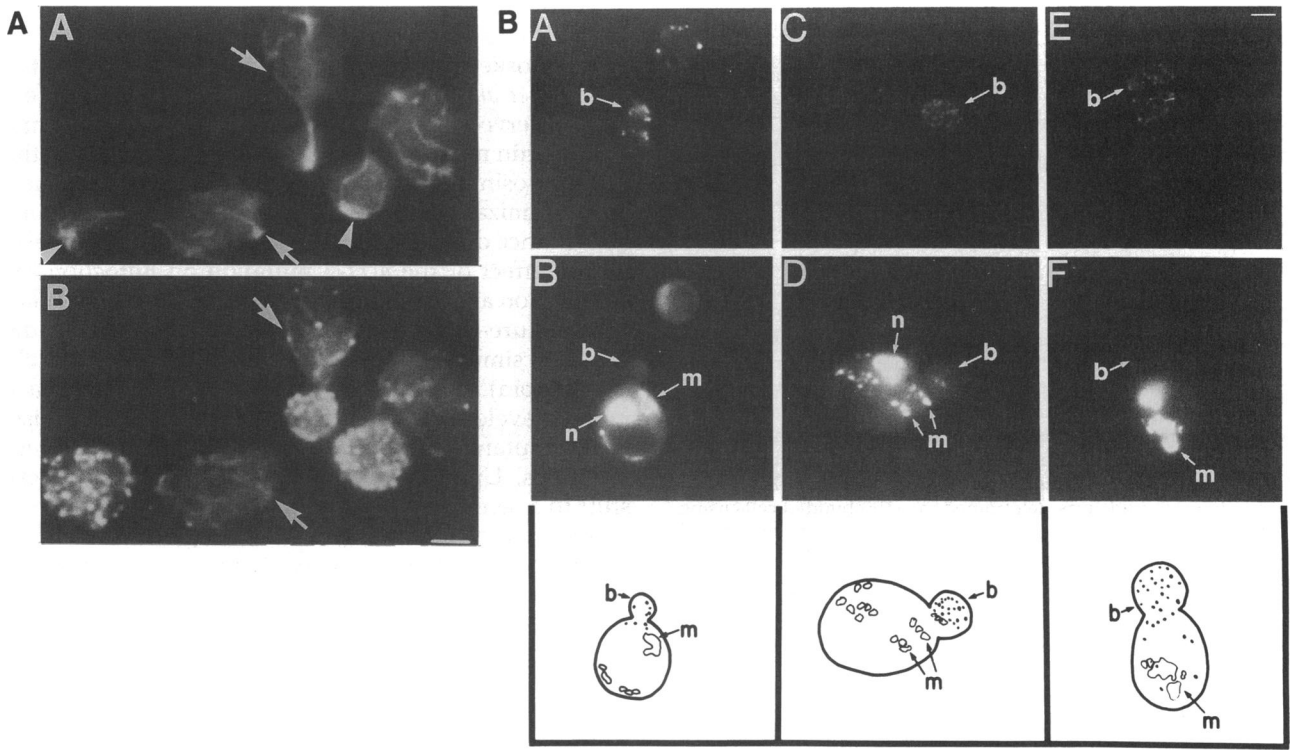

Figure 9. Effect of the *act1-3* mutation on mitochondrial inheritance. (A) *KWY474*, a yeast strain bearing the wild-type actin gene, was grown to midlog phase in YPD at 29°C. Cells were then fixed and converted to spheroplasts as for Figure 8. Mitochondria and microfilament-containing structures were visualized in the same cells by indirect immunofluorescence using antibodies raised against total mitochondrial outer membrane proteins (A) and the F-actin-specific stain rhodamine-phalloidin (B). Arrowheads highlight enrichment of mitochondria at bud tips. Arrows point to examples of mitochondria that align along actin cables. Bar, 1.8 μm. (B) The temperature-sensitive actin mutant, *act1-3* (*KWY230*), was grown to mid-to-late log phase in YPD at a semipermissive temperature (29°C). Cells were then fixed and converted to spheroplasts. Mitochondria (bottom) were visualized using DAPI. Actin patches that are present at the bud neck and enriched in the bud (top) were visualized in the same cells using rhodamine-coupled phalloidin. The drawings combine the actin and mitochondrial staining from panels directly above. Actin patches are depicted in black, and mitochondria are outlined. m, mitochondrial DNA; b, bud; n, nucleus. Bar, 1.5 μm.

addition, short-term incubation at 30°C resulted in even greater defects in the transfer process. These defects in mitochondrial inheritance occur in actin mutants grown on lactate or glucose-containing liquid media.

DISCUSSION

Using sedimentation assays, we find that isolated yeast mitochondria bind to phalloidin-stabilized yeast actin filaments and that the binding activity is ATP-sensitive, reversible, and saturable and therefore specific. Mitochondrial actin-binding activity is protease sensitive. Because loss of binding activity occurs under proteolytic conditions that degrade a mitochondrial outer membrane marker protein without affecting the integrity of the organelle, it is evident that actin-binding activity is mediated by a protein or proteins on the mitochondrial surface. Finally, saturation of myosin-binding sites on F-actin with the S1 subfragment of myosin blocks actin-mitochondrial interactions. Thus, our findings indicate that mitochondria bind to the lateral aspect of the microfilament.

Studies in many laboratories have identified and characterized ATP-sensitive protein-mediated actin-membrane interactions. Tranter *et al.* (1989, 1991) described an integral membrane protein with F- and G-actin–binding activity in rat liver membranes. Although this actin binding is ATP-sensitive, dose dependent, and saturable, it is irreversible; actin that is bound to the protein is not released by ATP. Members of the myosin superfamily have also been implicated in ATP-sensitive membrane-actin association. Early studies indicate that myosins display high and low affinity actin-binding. The ATP-bound state has low affinity for actin and the ATP-free and ADP-bound forms bind actin with high affinity. Myosins have actin-activated ATPase activity and readily convert between the high and low affinity actin-binding states. Thus, in contrast to the rat liver actin-binding protein described above, myosins display reversible, ATP-sensitive binding to actin (Warrick and Spudich, 1987; Kiehart, 1990; Titus, 1993). Other studies

Table 1. Mitochondrial inheritance defects in the *act1-3* mutant

Genotype	Temperature (°C)	Buds containing mitochondria (%)	
		YPD	Lactate medium
ACT1	22	83.8	96.9
act1-3	22	70.1	66.7
ACT1	30	87.8	91.7
act1-3	30	53.0	50.0

Tetrad analysis of *Act1/act1-3* diploids revealed segregation of mitochondrial distribution defects with the temperature-sensitive actin mutation. The effect of temperature on mitochondrial inheritance was examined in wild-type and temperature-sensitive sisters produced during tetrad analysis. Haploids were grown to midlog phase in YPD or lactate medium at 22°C. Aliquots of the culture were then incubated at 22 or 30°C for 45 min. Cells were fixed, converted to spheroplasts, and stained with the DNA binding dye DAPI, as above. Transfer of mitochondria into buds was determined in >100 budded cells using UV illumination to visualize mitochondria and nuclei, and bright field to visualize the boundaries of the mother cell and bud. Mitochondrial inheritance was measured by determining the percentage of the total budded cells that contain mitochondrial DNA within the small and medium-sized buds.

have identified membrane binding domains on some myosin isoforms (Pollard *et al.*, 1991) and shown that myosin-like proteins are present on the surface of microfilament-associated organelles and particles (Burridge and Phillips, 1975; Grolig *et al.*, 1988; Fath and Burgess, 1993). Finally, Adams and Pollard (1986) have obtained evidence that myosins mediate organelle-microfilament interactions and ATP-dependent movement of *Acanthamoeba* organelles along *Nitella* microfilaments. Thus, there is also extensive evidence for ATP-sensitive and reversible membrane-microfilament interactions that are mediated by membrane-associated myosin.

Several observations imply that mitochondria-microfilament interactions detected in this study are mediated by a myosin-like protein. First, many of the properties of mitochondrial-microfilament interactions are similar to those of myosin-F-actin interactions. Both processes are ATP-sensitive, reversible, and occur by association of a protein with the lateral surface of F-actin. In addition, myosin activity requires critical concentrations of Mg^{+2}-ATP (Weber, 1969; Reuben *et al.*, 1971). The concentration of ATP required for relaxation of skinned muscle fibers and for myosin-I motor activity is similar to that required for the ATP-sensitive actin-mitochondrial interactions detected here. In all cases, the minimum ATP concentration required is less than maximal cytosolic ATP levels. Finally, we observe that pretreatment of F-actin with myosin S1 subfragment blocks mitochondrial-actin interactions. Although we cannot rule out steric effects, it is possible that the myosin subfragment may be acting as a competitive inhibitor to block mitochondrial-actin binding activity.

Phenotypic analysis of *ACT1* mutants bearing charged-to-alanine substitutions suggests a role for the actin cytoskeleton in control of mitochondrial position (Drubin *et al.*, 1993). Because the most severe defects were observed upon mutation of the myosin "footprint" on the actin monomer, Drubin *et al.* (1993) propose that actin-myosin interactions might underlie the mitochondrial organization in yeast. Our studies of the functional significance of actin-mitochondrial interactions focused on the effect of the *act1-3* mutation on mitochondrial distribution and inheritance. The actin mutation displays temperature-dependent defects in mitochondrial distribution similar to those observed in other actin alleles (vide supra). In addition, transfer of mitochondria to newly developed buds during mitosis is compromised in the mutant even during growth at permissive temperatures. Upon continuous growth at or short term shift to a semipermissive temperature, the efficiency of mitochondrial inheritance is further decreased. Thus, the actin mutant also displays temperature-dependent defects in mitochondrial inheritance.

Because the *act1-3* mutation is known to have pleiotropic effects, it is possible that the defect in mitochondrial inheritance is an indirect effect. Several findings support a direct role for the actin cytoskeleton in the control of mitochondrial position and inheritance. First, actin that is specifically associated with mitochondria copurifies with the organelle during subcellular fractionation. In addition, fluorescence microscopy of dividing yeast cells reveals alignment of some mitochondria along actin cables (Drubin *et al.*, 1993) (Figure 9A). Other studies indicate that transfer of mitochondria into buds during cell division is extremely sensitive to the *act1-3* mutation. Mitochondrial inheritance is compromised in the actin mutant under permissive and semipermissive conditions where there is little to no mitochondrial aggregation and no significant effect on actin patch formation and localization within buds. Thus, the transfer defect is not simply a consequence of the mitochondrial aggregation. In addition, although actin cable formation is also impaired under these conditions, other actin dependent processes including bud formation and enlargement, enrichment of actin patches in buds, and cytokinesis are not significantly affected. This finding, that mitochondrial inheritance is more sensitive to actin mutation than other actin dependent processes, is consistent with the idea that mitochondrial inheritance defects are not pleiotropic effects of the actin mutation.

Considered together, our findings imply that a myosin-like protein(s) on mitochondrial surface mediates binding of the organelle to the yeast actin cytoskeleton, and that one consequence of this interaction may be control of mitochondrial position and inheritance during vegetative (mitotic) growth. Because destabilization of microtubules has no significant effect on mitochondrial movements during vegetative growth (Huffacker *et al.*, 1988), it appears that actin-mediated

mitochondrial movement is a major mechanism for control of mitochondrial spatial arrangement in vegetative yeast. Whether it is the sole mechanism for mitochondrial spatial control remains to be determined. It is possible that microtubules and other cytoskeletal networks affect mitochondria during other stages of the mitotic and/or meiotic cell cycle. In fact, recent evidence from McConnell and Yaffe (1992, 1993) suggests a role for an intermediate filament-like protein in control of mitochondrial inheritance in yeast. Because actin-, intermediate filament-, and microtubule-mediated organelle motility have been documented in many cells and because both actin and microtubule networks control organelle motility within the squid axon, it is clear that different cytoskeleton-based organelle motility systems are not mutually exclusive.

ACKNOWLEDGMENTS

We would like to thank D. Drubin, K. Wertman, L. Symington, J. Lessard, R. Schekman, H. Riezman, and G. Schatz for yeast strains, antibodies, suggestions, and shared unpublished observations. Support, shared equipment, and invaluable advice throughout this study were provided by R. Ambron, P. Brandt, J.C. Bulinski, J. Franke, R.H. Kessin, R. Liem, and A.J. Silverman. Finally, this work could not have been done without the expert technical assistance of Kathy Park and Beth Prairie. This work was supported by an award from the Short Term Training: Students in Health Professional Schools Program from the NIH to J.R. (5T35 HL-07616), as well as Training, Biomedical Research Support, and Research Grants (2T32 NS-07062, SO7 RR-05395, and RO1 GM-45735) from the NIH, Junior Faculty Research and Research Awards (ACS JFRA-377 and ACS CB-41) from the American Cancer Society, a Grant-in-aid Award (AHA CU50706601) from the American Heart Association, and the Basil O'Connor Starter Scholar Research Award (MDBDF #5-FY92-1143) from the March of Dimes.

REFERENCES

Adams, R.J., and Pollard, T.D. (1986). Propulsion of organelles isolated from *Acanthamoeba* along actin filaments by myosin-I. Nature *322*, 754–756.

Adams, A.E.M., and Pringle, J.R. (1984). Relationship of actin and tubulin distribution to bud growth in wild-type and morphogenetic-mutant *Saccharomyces cerevisiae*. J. Cell Biol. *98*, 934–945.

Albanesi, J.P., Fujisaki, J., Hammer, J.A., III, Korn, E.D., Jones, R., and Sheetz, M.P. (1985). Monomeric *Acanthamoeba* myosins-I support movement in vitro. J. Biol. Chem. *260*, 8649–8652.

Baker, D., and Schekman, R. (1989). Reconstitution of protein transport using broken yeast spheroplasts. Methods Cell Biol. *31*, 127–141.

Burridge, K., and Phillips, J.H. (1975). Association of actin and myosin with secretory granule membranes. Nature *254*, 526–529.

Chowdhury, S., Smith, K.W., and Gustin, M.C. (1992). Osmotic stress and the yeast cytoskeleton: phenotype-specific suppression of an actin mutation. J. Cell Biol. *118*, 561–571.

Cooper, J.A. (1987). Effects of cytochalasin and phalloidin on actin. J. Cell Biol. *105*, 1473–1478.

Daum, G., Boehni, P.C., and Schatz, G. (1982). Import of proteins into mitochondria: cytochrome b_2 and cytochrome c peroxidase are located in the intermembrane space of yeast mitochondria. J. Biol. Chem. *257*, 13028–13033.

Davis, L., and Blobel, G. (1986). Identification and characterization of a nuclear pore complex protein. Cell *45*, 699–709.

Drubin, D.G., Jones, H.D., and Wertman, K.F. (1993). Actin structure and function: roles in mitochondrial organization and morphogenesis in budding yeast and identification of the phalloidin-binding site. Mol. Biol. Cell *4*, 1277–1294.

Drubin, D.G., Miller, K.G., and Botstein, D. (1988). Yeast actin-binding proteins: evidence for a role in morphogenesis. J. Cell Biol. *107*, 2551–2561.

Fath, K.R., and Burgess, D.R. (1993). Golgi-derived vesicles from developing epithelial cells bind actin filaments and possess myosin-I as a cytoplasmically oriented peripheral membrane protein. J. Cell Biol. *120*, 117–127.

Govindan, B., Bowser, R., and Novick, P. (1991). Role of the unconventional myosin gene *MYO2* in the yeast secretory pathway. J. Cell Biol. *115*, 185a.

Greer, C., and Schekman, R. (1982). Actin from *Saccharomyces cerevisiae*. Mol. Cell. Biol. *2*, 1270–1278.

Grolig, F., Williamson, R.E., Parke, J., Miller, C., and Anderton, B.H. (1988). Myosin and calcium-sensitive streaming in the alga *Chara:* detection of two polypeptides reacting to a monoclonal anti-myosin and their localization in the streaming endoplasm. Eur. J. Cell Biol. *47*, 22–31.

Harlow, E., and Lane, D. (1988). Antibodies, A Laboratory Manual, Cold Spring Harbor, NY: Cold Spring Harbor Laboratory.

Hegmann, T.E., Lin, J.L., and Lin, J.J. (1990). Probing the role of non-muscle tropomyosin isoforms in intracellular granule movement by microinjection of monoclonal antibodies. J. Cell Biol. *109*, 1141–1152.

Hegmann, T.E., Schulte, D.L., Lin, J.L., and Lin, J.J. (1991). Inhibition of intracellular granule movement by microinjection of monoclonal antibodies against caldesmon. Cell Motil. Cytoskeleton *20*, 109–120.

Heuser, J.E., and Morisaki, J.H. (1992). Time-lapse video microscopy of endosomal "rocketing" in La/Zn treated cells. Mol. Biol. Cell *3*, 172a.

Holmes, K.C., Popp, D., Gebhard, W., and Kabsch, W. (1990). Atomic model of the actin filament. Nature *347*, 44–49.

Huffaker, T.C., Thomas, J.H., and Botstein, D. (1988). Diverse effects of beta-tubulin mutations on microtubule formation and function. J. Cell Biol. *106*, 1997–2010.

Johnston, G.C., Prendergast, J.A., and Singer, R.A. (1991). The *Saccharomyces cerevisiae MYO2* gene encodes an essential myosin for vectorial transport of vesicles. J. Cell Biol. *113*, 539–551.

Kachar, B. (1985). Direct visualization of organelle movement along actin filaments dissociated from *Characean* algae. Nature *227*, 1355–1357.

Kachar, B., and Reese, T.S. (1988). The mechanism of cytoplasmic streaming in *Characean* algal cells: sliding of endoplasmic reticulum along actin filaments. J. Cell Biol. *106*, 1545–1552.

Kiehart, D.P. (1990). Molecular genetic dissection of myosin heavy chain function. Cell *60*, 347–350.

Kilmartin, J.V., and Adams, A.E.M. (1984). Structural rearrangements of tubulin and actin during the cell cycle of the yeast *Saccharomyces*. J. Cell Biol. *98*, 922–933.

Kron, S.J., Drubin, D.G., Botstein, D., and Spudich, J.A. (1992). Yeast actin filaments display ATP-dependent sliding movement over surfaces coated with rabbit skeletal muscle myosin. Proc. Natl. Acad. Sci. USA *89*, 4466–4470.

Kuznetsov, S.A., Langford, G.M., and Weiss, D.G. (1992). Actin-dependent organelle movement in squid axoplasm. Nature *356*, 722–725.

Laemmli, U.K. (1970). Cleavage of structural proteins during the assembly of the head of bacteriophage T4. Nature *227*, 680–685.

Lessard, J.L. (1988). Two monoclonal antibodies to actin: one generally reactive and one muscle selective. Cell Motil. Cytoskeleton *10*, 349–362.

McConnell, S.J., Stewart, L.C., Talin, A., and Yaffe, M. (1990). Temperature-sensitive yeast mutants defective in mitochondrial inheritance. J. Cell Biol. *111*, 967–976.

McConnell, S.J., and Yaffe, M.P. (1992). Nuclear and mitochondrial inheritance in yeast depends on novel cytoplasmic structure defined by the *MDM1* protein. J. Cell Biol. *118*, 385–395.

McConnell, S.J., and Yaffe, M.P. (1993). Intermediate filament formation by a yeast protein essential for organelle inheritance. Science *260*, 687–689.

Ng, R., and Abelson, J. (1980). Isolation and sequence of the gene for actin in *Saccharomyces cerevisiae*. Proc. Natl. Acad. Sci. USA *77*, 3912–3916.

Novick, P., and Botstein, D. (1985). Phenotypic analysis of temperature-sensitive yeast actin mutants. Cell *40*, 405–416.

Nuoffer, C., Horvath, A., and Riezman, H. (1993). Analysis of the sequence requirement for glycosylphosphatidylinositol anchoring of *Saccharomyces cerevisiae Gas1* protein. J. Cell Biol. *268*, 10558–10563.

Palmer, R.E., Sullivan, D.S., Huffaker, T., and Koshland, D. (1992). Role of astral microtubules and actin in spindle orientation and migration in the budding yeast, *Saccharomyces cerevisiae*. J. Cell Biol. *119*, 583–593.

Pollard, T.D., Doberstein, S.K., and Zot, H.G. (1991). Myosin-I. Annu. Rev. Physiol. *53*, 653–681.

Pon, L.A., Moll, T., Vestweber, D., Marshallsay, B., and Schatz, G. (1989). Protein import into mitochondria: demonstration of ATP-dependent translocation activity in a submitochondrial fraction enriched in membrane contact sites and specific proteins. J. Cell Biol. *109*, 2603–2616.

Pringle, J.R., Preston, R.A., Adams, A.E.M., Sterns, T., Drubin, D.G., Haarer, B.K., and Jones, E.W. (1989). Fluorescence microscopy methods for yeast. Methods Cell Biol. *31*, 357–435.

Read, E.B., Okamura, H.H., and Drubin, D.G. (1992). Actin- and tubulin-dependent functions during *Saccharomyces cerevisiae* mating projection formation. Mol. Biol. Cell *3*, 429–444.

Reuben, J.P., Brandt, P.W., Berman, M., and Grundfest, H. (1971). Regulation of tension in the skinned crayfish muscle fiber. J. Gen. Physiol. *57*, 385–407.

Riezman, H. (1993). Yeast endocytosis. Trends Cell Biol. *3*, 273–277.

Riezman, H., Hay, R., Gasser, S., Daum, G., Schneider, G., Witte, C., and Schatz, G. (1983). The outer membrane of yeast mitochondria: isolation of outside-out sealed vesicles. EMBO J. *2*, 1105–1111.

Sheetz, M.P., and Spudich, J.A. (1983). Movement of myosin-coated fluorescent beads on actin cables in vitro. Nature *303*, 31–35.

Sherman, F. (1991). Getting started with yeast. Methods Enzymol. *194*, 3–37.

Shortle, D., Haber, J.E., and Botstein, D. (1982). Lethal disruption of the yeast actin gene by integrative DNA transformation. Science *217*, 371–373.

Shortle, D., Novick, P., and Botstein, D. (1984). Construction and genetic characterization of temperature-sensitive mutant alleles of the yeast actin gene. Proc. Natl. Acad. Sci. USA *81*, 4889–4893.

Sreter, F., Holtzer, S., Gergely, J., and Holzter, J. (1972). Some properties of embryonic myosin. J. Cell Biol. *55*, 586–594.

Stevens, B.J. (1977). Variation in number and volume of the mitochondria in yeast according to growth conditions. A study based on serial sectioning and computer graphics reconstitution. Biol. Cell *28*, 37–56.

Stevens, B. (1981). Mitochondrial structure. In: The Molecular Biology of the Yeast *Saccharomyces:* Life Cycle and Inheritance, eds. J.N. Strathern, E.W. Jones, and J.R. Broach, Cold Spring Harbor, NY: Cold Spring Harbor Laboratory, 471–488.

Stirling, C.J., Rothblatt, J., Hosobuchi, M., Deshaies, R., and Schekman, R. (1992). Protein translocation mutants defective in the insertion of integral membrane proteins into the endoplasmic reticulum. Mol. Biol. Cell *3*, 129–142.

Theriot, J.A., Mitchison, T.J., Tilney, L.G., and Portnoy, D.A. (1992). The rate of actin-based motility of intracellular *Listeria monocytogenes* equals the rate of actin polymerization. Nature *357*, 257–260.

Thomas, J.H., and Botstein, D. (1986). A gene required for the separation of chromosomes on the spindle apparatus in yeast. Cell *44*, 65–76.

Tilney, L.G., DeRosier, D.J., and Tilney, M.S. (1992a). How *Listeria* exploits host cell actin to form its own cytoskeleton. I. Formation of a tail and how that tail might be involved in movement. J. Cell Biol. *118*, 71–81.

Tilney, L.G., DeRosier, D.J., Weber, A., and Tilney, M.S. (1992b). How *Listeria* exploits host cell actin to form its own cytoskeleton. II. Nucleation, actin filament polarity, filament assembly, and evidence for a pointed end capper. J. Cell Biol. *118*, 83–93.

Titus, M.A. (1993). Myosins. Curr. Opin. Cell Biol. *5*, 77–81.

Towbin, H., Staehelin, T., and Gordon, J. (1979). Electrophoretic transfer of proteins from polyacrylamide to nitrocellulose sheets: procedure and some applications. Proc. Natl. Acad. Sci. USA *76*, 4350–4354.

Tranter, M.P., Sugrue, S.P., and Schwartz, M.A. (1989). Evidence for a direct, nucleotide-sensitive interaction between actin and liver cell membranes. J. Cell Biol. *109*, 2833–2840.

Tranter, M.P., Sugrue, S.P., and Schwartz, M.A. (1991). Binding of actin to liver cell membranes: the state of membrane-bound actin. J. Cell Biol. *112*, 891–901.

Tzagoloff, A. (1982). Mitochondria, New York: Plenum Press.

Warrick, H.M., and Spudich, J.A. (1987). Myosin structure and function in cell motility. Annu. Rev. Cell Biol. *3*, 379–421.

Weber, A. (1969). Parallel response of myofibrillar contraction and relaxation to four different nucleoside triphosphates. J. Gen. Physiol. *53*, 781–791.

Weeds, A.G., and Taylor, R.S. (1975). Separation of subfragment-1 isoenzymes from rabbit skeletal muscle myosin. Nature *257*, 54–56.

Wessels, D., Schroeder, N.A., Voss, E., Hall, A.L., Condeelis, J., and Soll, D.R. (1989). cAMP-mediated inhibition of intracellular particle movement and actin reorganization in *Dictyostelium*. J. Cell Biol. *109*, 2841–2851.

Wessels, D., and Soll, D.R. (1990). Myosin II heavy chain null mutant of *Dictyostelium* exhibits defective intracellular particle movement. J. Cell Biol. *111*, 1137–1148.

Williamson, D.H., and Fennell, D.J. (1975). The use of fluorescent DNA-binding agent for detecting and separating yeast mitochondrial DNA. Methods Cell Biol. *12*, 335–351.

Vibert, P., and Cohen, C. (1988). Domains, motion and regulation in the myosin head. J. Muscle Res. Cell Motil. *9*, 296–304.

Zechel, K. (1980). Isolation of polymerization competent cytoplasmic actin by affinity chromatography on immobilized DNase 1 using formamide as an eluant. Eur. J. Biochem. *110*, 343–348.